

Accuracy of washout rate analysis for thallium-201 single-photon emission computed tomography myocardial perfusion imaging using cadmium zinc telluride detectors: A phantom study

JRSM Cardiovascular Disease

Volume 9: 1–5

© The Author(s) 2020

Article reuse guidelines:

sagepub.com/journals-permissions

DOI: 10.1177/2048004019900600

journals.sagepub.com/home/cvd

Masaru Ishihara¹ , Masahisa Onoguchi² and Takayuki Shibutani²

Abstract

Objective: The aim of this study was to assess the accuracy of washout rate (WOR) analysis for thallium-201 chloride (²⁰¹Tl) single-photon emission computed tomography myocardial perfusion imaging data acquired using cadmium zinc telluride detectors and a myocardial phantom.

Methods: A myocardial phantom was injected with 10.5 MBq ²⁰¹Tl, and 10-min acquisitions were performed at 0, 24, 46, and 62 h to accommodate natural radioactive decay over time. Global myocardial WOR (global-WOR) and regional WOR (regional-WOR, left anterior descending artery [LAD], right coronary artery [RCA], and left circumflex artery [LCX]) were analyzed between 0 and 24 h (infarction model), 0 and 46 h (ischemia model), and 0 and 62 h (normal model), respectively. We compared the calculated radioactive decay-rate as a reference standard and phantom imaging WOR (phantom-WOR).

Results: Decay-rate versus phantom-WOR were 20.4% vs. 20.8% (global-WOR), 21.3% (LAD), 21.2% (RCA), and 19.7% (LCX) for the infarction model; 35.4% vs. 35.6% (global-WOR), 35.5% (LAD), 36.2% (RCA), and 35.2% (LCX) for the ischemia model; and 44.5% vs. 45.1% (global-WOR), 45.4% (LAD), 44.7% (RCA), and 43.5% (LCX) for the normal model.

Conclusion: WOR analysis for ²⁰¹Tl single-photon emission computed tomography myocardial perfusion imaging using cadmium zinc telluride detectors is a reliable analysis method.

Keywords

Thallium-201 chloride, single-photon emission computed tomography, washout rate, cadmium zinc telluride detectors

Date received: 17 May 2019; revised: 12 November 2019; accepted: 16 December 2019

Introduction

Thallium-201 chloride (²⁰¹Tl) is widely used as a single-photon emission computed tomography (SPECT) myocardial perfusion imaging (MPI) agent. ²⁰¹Tl SPECT allows for noninvasive evaluation of coronary artery disease (CAD).^{1,2}

In ²⁰¹Tl SPECT MPI, regional hypoperfusion can be evaluated using short-axis, vertical long-axis, and horizontal long-axis images. However, global hypoperfusion in myocardial ischemia (balanced ischemia and diffuse abnormal flow reserve) might be underestimated.^{3,4} Washout rate (WOR) analysis for ²⁰¹Tl SPECT MPI can help detect abnormalities in patients with apparently normal MPI.^{5–7} For clinical use, it is

important to confirm the accuracy of WOR analysis for ²⁰¹Tl SPECT MPI.

The aim of this study was to assess the accuracy of WOR analysis for ²⁰¹Tl SPECT MPI data acquired

¹Department of Radiology, Hyogo Cancer Center, Hyogo, Japan

²Department of Quantum Medical Technology, Graduate School of Medical Sciences, Kanazawa University, Ishikawa, Japan

Corresponding author:

Masaru Ishihara, Department of Radiology, Hyogo Cancer Center, 13-70 Kitaoji, Akashi, Hyogo 673-8558, Japan.

Email: hbhcishihara@gmail.com



using cadmium zinc telluride (CZT) detectors and a myocardial phantom.

Methods

A scanner with CZT detectors (D-SPECT cardiac scanner; Spectrum Dynamics, Caesarea, Israel) and a myocardial phantom (RH-2; Kyoto-Kagaku, Kyoto, Japan) were used. The phantom (Figure 1) was injected with 10.5 MBq ^{201}Tl , and 10-min acquisitions were performed at 0, 24, 46, and 62 h to accommodate natural radioactive decay over time. Natural radioactive decay over time was used to calculate radioactivity, and the WOR for the abnormal model was $<40\%$.⁸ For the calculation analysis of the basic WOR, the first myocardial counts (stress imaging in clinical cases) and decreased second myocardial counts, due to physiological washout over time (redistribution imaging in clinical cases), were used. In our phantom study, myocardial counts at 24, 46, and 62 h were measured due to natural decay.

Imaging was conducted using an energy peak and energy window width of $71 \text{ keV} \pm 15\%$. For all acquisitions, the raw projection data were reconstructed using an iterative maximum likelihood expectation maximization algorithm (ML-EM) using a variant of the ordered-subset expectation maximization algorithm (OS-EM) using three and four iterations and 32 subsets.⁹ The WORs were analyzed between 0 and 24 h (infarction model), 0 and 46 h (ischemia model), and 0 and 62 h (normal model) (Figure 2) using the scanner's software (D-SPECT WOR Software, Spectrum Dynamics, Caesarea, Israel). D-SPECT WOR software decay correction was not employed during WOR analysis in this study, and natural decay was used to

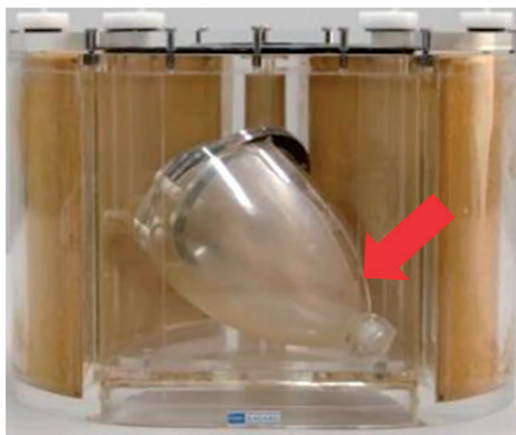


Figure 1. Photograph showing the myocardial phantom and thallium-201 chloride (^{201}Tl) injection site (arrow) in the myocardial area (187 mL).

calculate the WOR because decay correction underestimates the WOR.

The formula for calculating radioactivity from the images at 0, 24, 46, and 62 h was

$$N = N_0(1/2)^{t/T}$$

where N = radioactivity at time t , N_0 = initial radioactivity, t = time (h), $T = 72.97$ h. The formula for decay-rate in the infarction model, ischemia model, and normal model was

$$\text{WOR}(\%) = [(N_0 - N]/N_0) \times 100$$

The same formula was used to calculate the WOR in all models.

The initial (N_0) radioactivity in the myocardial phantom was 10.5 MBq. The 24 h (N_{24}) radioactivity of the myocardial phantom was 8.4 MBq ($= N_0[1/2]^{24.00/72.97}$), 46 h (N_{46}) radioactivity of the myocardial phantom was 6.8 MBq ($= N_0[1/2]^{46.00/72.97}$), and 62 h (N_{62}) radioactivity of the myocardial phantom was 5.8 MBq ($= N_0[1/2]^{62.00/72.97}$). The 0–24 h decay-rate was 20.4% ($= [(N_0 - N_{24})/N_0] \times 100$), 0–46 h decay-rate was 35.4% ($= [(N_0 - N_{46})/N_0] \times 100$), and 0–62 h decay-rate was 44.5% ($= [(N_0 - N_{62})/N_0] \times 100$).^{8,10}

Differences between the decay-rate as a reference standard and the phantom imaging WOR (phantom-WOR) were compared. Phantom-WORs were used for the global myocardial WOR (global-WOR) and coronary artery regions (regional-WOR). All WORs were automatically calculated using the D-SPECT WOR software. Regional-WORs were divided into three main territories: left anterior descending artery (LAD), right coronary artery (RCA), and left circumflex artery (LCX). The left ventricle was divided into 17 segments using the American Heart Association model¹¹ with the LAD supplying segments 1, 2, 7, 8,

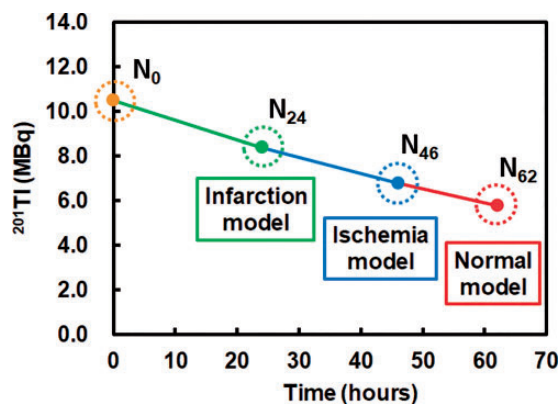


Figure 2. Models of ^{201}Tl for various levels of myocardial blood flow: infarction model (N_0 – N_{24}), ischemia model (N_0 – N_{46}), and normal model (N_0 – N_{62}).

13, 14, and 17; RCA supplying segments 3, 4, 9, 10, and 15; and LCX supplying segments 5, 6, 11, 12, and 16.

Statistical analyses were performed using spreadsheet software (Microsoft Excel 2016, Microsoft Corp., Redmond WA, USA). The error was obtained as the absolute error. It is shown as follows:

$$\text{Absolute error} = |(\text{phantom} - \text{WOR}) - (\text{decay} - \text{rate})|$$

Table 1. Global-WOR values.

	Infarction model	Ischemia model	Normal model
Decay-rate (%)	20.4	35.4	44.5
Phantom-WOR (%)	20.8	35.6	45.1
Absolute error (%)	0.4	0.2	0.6

Decay-rate: calculated natural radioactive decay rate; Phantom-WOR: phantom imaging washout rate

Table 2. Regional-WOR values.

	Infarction model			Ischemia model			Normal model		
	LAD	RCA	LCX	LAD	RCA	LCX	LAD	RCA	LCX
Decay-rate (%)	20.4			35.4			44.5		
Phantom-WOR (%)	21.3	21.2	19.7	35.5	36.2	35.2	45.4	44.7	43.5
Absolute error (%)	0.9	0.8	0.7	0.1	0.8	0.2	0.9	0.2	1.0

LAD: left anterior descending artery, RCA: right coronary artery, LCX: left circumferential artery, Decay-rate: calculated natural radioactive decay rate; Phantom-WOR: phantom imaging washout rate

Results

The reconstructed myocardial counts were 2.44 million at 0 h, 1.92 million at 24 h, 1.54 million at 46 h, and 1.33 million at 62 h. Decay-rate, phantom-WOR, and absolute error for each model are shown in Tables 1 and 2. Absolute error ranged from 0.2% to 0.6% for global-WOR, and from 0.1% to 1.0% for regional-WOR.

Phantom-WOR images are shown in Figure 3.

Discussion

Recently, dedicated cardiac systems with CZT detectors were introduced in Japan. The improvements in efficiency and resolution allow low-dose imaging protocols, reduce the acquisition time, and permit quantification of the myocardial perfusion reserve using dynamic SPECT images.^{12–14} ²⁰¹Tl is widely used for SPECT MPI in many Asian countries. ²⁰¹Tl SPECT

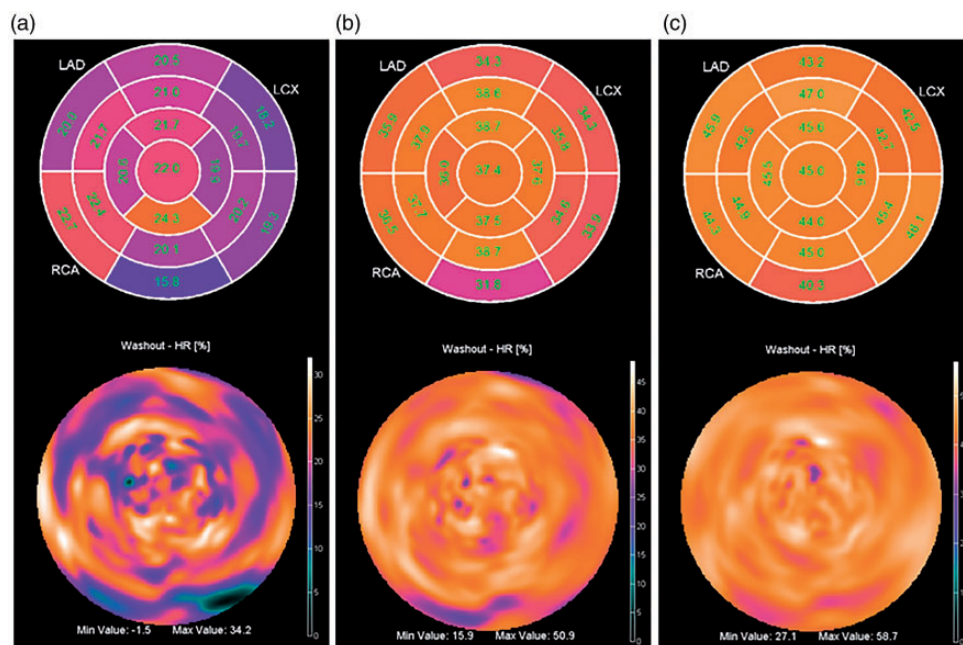


Figure 3. Phantom-WOR analysis images of ²⁰¹Tl SPECT MPI: infarction model (a), ischemia model (b), and normal model (c).

MPI WOR is also a valuable tool when diagnosing CAD.^{7,15} There are methods of calculating WOR from planar and SPECT images.^{15–17} In this study, we used CZT detectors and a myocardial phantom and assessed the accuracy of WOR analysis for ²⁰¹Tl SPECT MPI.

We observed the natural radioactive decay that occurs over time and created an infarction model, ischemia model, and normal model. In our previous study,¹⁸ ²⁰¹Tl SPECT MPI required a counts of ≥ 1.2 million. Therefore, the myocardial counts at 0 h were ≥ 2.20 million, and at 62 h (used for the normal model) were calculated to be ≥ 1.20 million, with an acquisition time set to 10-min in this study (to record natural radioactive decay).

In clinical cases, the decrease in reproducibility can be due to repositioning effects between the first and second acquisitions. A previous study showed that reproducibility was unaffected by the myocardial phantom and clinical cases in several instances.¹⁹ In the present study, inaccuracy of misalignment was controlled for by keeping the CZT detectors and the myocardial phantom immobile over acquisitions performed at 24, 46, and 62 h.

We found an absolute error of decay-rate and phantom-WOR for both global-WOR and regional-WOR to be $\leq 1.0\%$, with excellent accuracy of the WOR analysis results.

This study elucidated the accuracy of the WOR using the new CZT system. In the future, it is expected to have clinical application in the diagnosis of disease, especially multivessel disease and slightly abnormal myocardial perfusion.

Conclusion

The WOR analysis for ²⁰¹Tl SPECT MPI using CZT detectors is a reliable analysis method.

Acknowledgements

We thank the radiological technologists and cardiologists of Hyogo Brain and Heart Center at Himeji for technical support. We would like to thank Editage (www.editage.jp) for English language editing.

Contributors

MI and MO researched literature. All authors conceived the report. MI wrote the first draft of the article. All authors reviewed and edited the article and approved the final version.

Declaration of conflicting interests

The author(s) declared no potential conflicts of interest with respect to the research, authorship, and/or publication of this article.

Ethical approval

This work does not contain any studies with human participants or animals.

Funding

The author(s) received no financial support for the research, authorship, and/or publication of this article.


Guarantor

MI.

Informed consent

Not applicable.

ORCID iD

Masaru Ishihara  <https://orcid.org/0000-0001-7133-1972>

References

1. Chen CC, Huang WS, Hung GU, et al. Left-ventricular dyssynchrony evaluated by thallium-201 gated SPECT myocardial perfusion imaging: a comparison with Tc-99m sestamibi. *Nucl Med Commun* 2013; 34: 229–232.
2. Shiraishi S, Sakamoto F, Tsuda N, et al. Prediction of left main or 3-vessel disease using myocardial perfusion reserve on dynamic thallium-201 single-photon emission computed tomography with a semiconductor gamma camera. *Circ J* 2015; 79: 623–631.
3. Maddahi J, Garcia EV, Berman DS, et al. Improved non-invasive assessment of coronary artery disease by quantitative analysis of regional stress myocardial distribution and washout of thallium-201. *Circulation* 1981; 64: 924–935.
4. Berman DS, Kang X, Slomka PJ, et al. Underestimation of extent of ischemia by gated SPECT myocardial perfusion imaging in patients with left main coronary artery disease. *J Nucl Cardiol* 2007; 14: 521–528.
5. Bateman TM, Maddahi J, Gray RJ, et al. Diffuse slow washout of myocardial thallium-201: a new scintigraphic indicator of extensive coronary artery disease. *J Am Coll Cardiol* 1984; 4: 55–64.
6. Koskinen M, Pöyhönen L and Seppänen S. Thallium-201 washout in coronary artery disease using SPECT – a comparison with coronary angiography. *Eur J Nucl Med* 1987; 12: 609–612.
7. Yamada M, Chikamori T, Doi Y, et al. Negative washout rate of myocardial thallium-201 – a specific marker for high grade coronary artery narrowing. *Jpn Circ J* 1992; 56: 975–982.
8. Sata N, Tanaka Y, Toufuku K, et al. Low washout rate during stress thallium-201 myocardial scintigraphy. Transient left ventricular dysfunction in a patient with grant splenomegaly due to polycythemia vera. *J Cardiol* 2005; 46: 39–41.
9. Erlandsson K, Kacperski K, van Gramberg D, et al. Performance evaluation of D-SPECT: a novel SPECT

- system for nuclear cardiology. *Phys Med Biol* 2009; 54: 2635–2649.
10. Nishimura T, Uehara T, Hayashida K, et al. Quantitative assessment of thallium myocardial washout rate: importance of peak heart rate and lung thallium uptake in defining normal values. *Eur J Nucl Med* 1987; 13: 67–71.
 11. Cerqueira MD, Weissman NJ, Dilsizian V, et al. American Heart Association Writing Group on Myocardial Segmentation and Registration for Cardiac Imaging Standardized myocardial segmentation and nomenclature for tomographic imaging of the heart. A statement for healthcare professionals from the Cardiac Imaging Committee of the Council on Clinical Cardiology of the American Heart Association. *Circulation* 2002; 105: 539–542.
 12. Sharir T, Ben-Haim S, Merzon K, et al. High-speed myocardial perfusion imaging initial clinical comparison with conventional dual detector angler camera imaging. *JACC Cardiovasc Imag* 2008; 1: 156–163.
 13. Songy B, Lussato D, Guernou M, et al. Comparison of myocardial perfusion imaging using thallium-201 between a new cadmium-zinc-telluride cardiac camera and a conventional SPECT camera. *Clin Nucl Med* 2011; 36: 776–780.
 14. Ben-Haim S, Murthy VL, Breault C, et al. Quantification of myocardial perfusion reserve using dynamic SPECT imaging in humans: a feasibility study. *J Nucl Med* 2013; 54: 873–879.
 15. Ishihara M, Onoguchi M and Shibutani T. An exploratory study of washout rate analysis for thallium-201 single-photon emission computed tomography myocardial perfusion imaging using cadmium zinc telluride detectors. *Mol Imaging* 2018; 17: 1–6.
 16. Nakajima K, Verschure DO, Okuda K, et al. Standardization of ^{123}I -meta-iodobenzylguanidine myocardial sympathetic activity imaging: phantom calibration and clinical applications. *Clin Transl Imaging* 2017; 5: 255–263.
 17. Hayashi D, Ohshima S, Isobe S, et al. Increased $^{99\text{m}}\text{Tc}$ -sestamibi washout reflects impaired myocardial contractile and relaxation reserve during dobutamine stress due to mitochondrial dysfunction in dilated cardiomyopathy patients. *J Am Coll Cardiol* 2013; 61: 2007–2017.
 18. Ishihara M, Taniguchi Y, Onoguchi M, et al. Optimal thallium-201 dose in cadmium-zinc-telluride SPECT myocardial perfusion imaging. *J Nucl Cardiol* 2018; 25: 947–954.
 19. Backus BE, Verburg FA, Romijn RL, et al. Intra-patient reproducibility of myocardial SPECT imaging with ^{201}Tl . *J Nucl Cardiol* 2009; 16: 97–104.